Formation and Characterization of Mononuclear and Dinuclear Manganese Oxide-Dioxygen Complexes in Solid Argon

Yu Gong, Guanjun Wang, and Mingfei Zhou*

Department of Chemistry, Shanghai Key Laboratory of Molecular Catalysts and Innovative Materials, Advanced Materials Laboratory, Fudan University, Shanghai 200433, P. R. China

Received: February 1, 2008

A manganese atom reacts with dioxygen to form the previously characterized MnO_2 molecule in solid argon under UV−visible light irradiation. Subsequent sample annealing allows the dioxygen molecules to diffuse and to react with MnO_2 to give the $(\eta^2\text{-}O_2)MnO_2$ complex, which is characterized to be a side-on bonded peroxo manganese dioxide complex. The manganese tetraoxide MnO_4, which was predicted to be less stable than the $(\eta^2\text{-}O_2)MnO_2$ isomer, was not observed. However, the $(\eta^2\text{-}O_2)MnO_2$ complex reacts with another weakly coordinated dioxygen to give the $(\eta^2\text{-}O_2)MnO_4$ complex via visible light irradiation, in which the manganese tetraoxide is coordinated and stabilized by a side-on bonded O_2 molecule. Manganese dimer reacts with dioxygen to form the cyclic $Mn(\mu\text{-}O)_2Mn$ cluster spontaneously upon annealing, which further reacts with dioxygen to give the $(\eta^2\text{-}O_2)_2Mn(\mu\text{-}O)_2Mn$ cluster, a side-on bonded disuperoxide complex with a planar D_{2h} structure.

Introduction

Manganese oxides and dioxygen complexes play important roles in catalysis and in many biological systems. Simple manganese oxides such as MnO, MnO_2, and their anions have been well studied both experimentally[1–6] and theoretically.[7–11] Higher oxygen-rich manganese oxides have also been the subject of some investigations, but most efforts have been focused on the permanganate anion, MnO_4^-, a very common anion in solids and solutions, which is extensively used as an oxidizing agent.[12–20] It was characterized to possess a tetrahedral geometry with rather large electron-detachment energy.[13] Compared to the MnO_4^- anion, the neutral MnO_4 species has received much less attention. The ground state of manganese tetraoxide was determined to have a C_{3v} symmetry in an earlier matrix isolation electron spin resonance study.[5] Later investigation on the reactions of laser-ablated manganese atoms and O_2 was performed by using matrix isolation infrared (IR) spectroscopy. Two absorptions at 974.9 and 1130 cm^{-1} were assigned to the $(\eta^2\text{-}O_2)MnO_2$ complex in solid argon, which was characterized to be a side-on bonded superoxo manganese dioxide complex.[6] However, a combined first-principles theoretical and photoelectron spectroscopic study of MnO_4^- and MnO_4 in the gas phase revealed that the most stable configuration of the neutral MnO_4 molecule is a distorted tetraoxide with C_{2v} symmetry, in which all the oxygen atoms are atomically bound to the manganese center without direct O−O bonding.[13] Apparently, there are still some contradictions in the assignment of the MnO_4 species.

The structure, bonding, and reactivity of dinuclear manganese oxide clusters have also been investigated.[21–25] The Mn_2O cluster was identified to possess a high-spin state with ferromagnetic feature.[21] The ferromagnetic Mn_2O_2 cluster was regarded as building block for bulk manganese oxide and was characterized to have a rhombic structure.[6,22]

In this paper, the reaction of manganese atoms and dioxygen are reinvestigated by using matrix isolation IR absorption spectroscopy with lower laser energies and emission plume intensities. Some mononuclear and dinuclear manganese oxide−dioxygen complexes produced via the reactions of manganese atoms and dimers with dioxygen are assigned.

Experimental and Computational Methods

The experimental setup for pulsed laser evaporation and matrix isolation IR spectroscopic investigation has been described in detail previously.[26] Briefly, the 1064 nm fundamental of a Nd:YAG laser (Continuum, Minilite II, 10 Hz repetition rate and 6 ns pulse width) was focused onto a rotating manganese target through a hole in a CsI window cooled normally to 6 K by means of a closed-cycle helium refrigerator (ARS, 202N). The laser-evaporated metal atoms were codeposited with oxygen/argon mixtures onto the CsI window. In general, matrix samples were deposited for 1 to 1.5 h at a rate of approximately 4 mmol/h. The O_2/Ar mixtures were prepared in a stainless steel vacuum line by using standard manometric technique. Isotopic $^{18}O_2$ (ISOTEC, 99%) was used without further purification. The IR absorption spectra of the resulting samples were recorded on a Bruker IFS 66V spectrometer at 0.5 cm^{-1} resolution between 4000 and 450 cm^{-1} by using a liquid-nitrogen-cooled HgCdTe (MCT) detector. Samples were annealed to different temperatures and cooled back to 6 K for spectral acquisition, and selected samples were subjected to broadband irradiation by using a tungsten lamp or a high-pressure mercury arc lamp with glass filters.

Quantum chemical calculations were performed by using the Gaussian 03 program.[27] The three-parameter hybrid functional according to Becke with additional correlation corrections from Lee, Yang, and Parr (B3LYP) was utilized.[28] The 6-311+G* basis set was used for the oxygen atom, and the all-electron basis set of Wachters-Hay as modified by Gaussian was used for the Mn atom.[29] The geometries were fully optimized; the harmonic vibrational frequencies were calculated, and zero-point vibrational energies were derived. For selected species, the single-point energies of the structures optimized at the B3LYP level of theory were calculated by using the CCSD(T) method with the same basis set.

* E-mail: mfzhou@fudan.edu.cn.

10.1021/jp800955e CCC: $40.75
Published on Web 05/13/2008

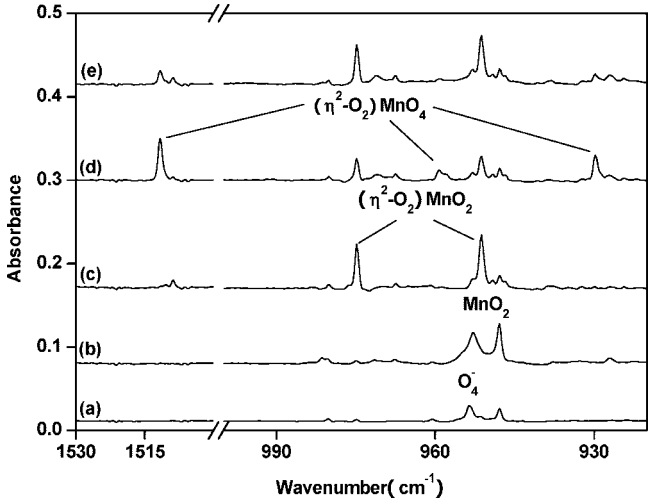

Figure 1. IR spectra in the 1530−1500 and 1000−920 cm^{-1} regions from codeposition of laser-evaporated manganese atoms with 1.0% O_2 in argon. (a) 1 h of sample deposition at 6 K, (b) after 15 min of 250 $< \lambda <$ 580 nm irradiation, (c) after 35 K annealing, (d) after 15 min of $\lambda >$ 500 nm irradiation, and (e) after 15 min of 300 $< \lambda <$ 580 nm irradiation.

Results and Discussion

IR Spectra. A series of experiments were performed by using different dioxygen concentrations and laser energies. The spectra in the O−O stretching and Mn−O stretching vibrational frequency regions from the experiment using 1.0% O_2 and approximately 5 mJ/pulse laser energy are shown in Figure 1, and the product absorptions are listed in Table 1. After 1 h of sample deposition at 6 K, product absorptions at 953.6, 948.0, 858.3, 833.1, and 816.4 cm^{-1} were observed. The 953.6 cm^{-1} absorption is common for laser-ablated metal atom reactions with dioxygen and has been previously assigned to the O_4^- anion absorption.[30] The 948.0 and 816.4 cm^{-1} absorptions were assigned to the antisymmetric and symmetric stretching vibrations of the inserted MnO_2 molecule.[6] The 858.3 cm^{-1} absorption is due to the MnO_2^- anion.[6,15] The 833.1 cm^{-1} absorption was initially assigned to the manganese monoxide,[6] but recent investigation revealed that the MnO molecule was coordinated by one argon atom, and this absorption should be regarded as the ArMnO complex instead of the isolated diatomic molecule.[31] The anion absorptions were bleached whereas the MnO_2 absorptions were strongly enhanced when the as-deposited sample was subjected to UV−visible light irradiation with the output of a high-pressure mercury arc lamp (Figure 1, trace b). When the sample was annealed to 35 K (Figure 1, trace c), two new absorptions at 974.8 and 951.3 cm^{-1} were produced at the expense of the MnO_2 absorptions. Subsequent visible light irradiation by using a tungsten lamp with a 500 nm long wavelength pass filter almost destroyed these two absorptions and produced three new absorptions at 1511.7, 959.2, and 929.8 cm^{-1} (Figure 1, trace d). Additional irradiation (300 $< \lambda <$ 580 nm) with a high-pressure mercury lamp with a 300 nm long wavelength pass filter recovered the 974.8 and 951.3 cm^{-1} absorptions at the expense of the 1511.7, 959.2, and 929.8 cm^{-1} absorptions (Figure 1, trace e).

Another experiment was performed with the same laser energy as that used in the experiment in Figure 1, but the sample was subjected to annealing directly after deposition instead of being exposed to UV−visible light irradiation. The MnO_2 absorptions as well as the 974.8 and 951.3 cm^{-1} absorptions are much weaker than those in Figure 1. However, two absorptions at 600.8 and 504.9 cm^{-1} which were previously[6] assigned to the cyclic Mn(μ-O)$_2$Mn cluster appeared and increased on annealing, as shown in Figure 2. In addition, two additional absorptions at 1092.0 and 683.6 cm^{-1} were produced after the Mn(μ-O)$_2$Mn absorptions when the sample was annealed to high temperatures.

Experiments were repeated by using the isotopic substituted $^{18}O_2$, $^{16}O_2 + {}^{18}O_2$, and $^{16}O_2 + {}^{16}O^{18}O + {}^{18}O_2$ samples to help with the product assignments. The band positions of the new product absorptions are summarized in Table 1. The spectra in selected regions with different isotopic samples are shown in Figures 3–5.

(η^2-O_2)MnO_2. The 974.8 cm^{-1} absorption corresponding to the absorption at 974.9 cm^{-1} was previously assigned to the antisymmetric MnO_2 stretching mode of the (η^2-O_2)MnO_2 complex.[6] The isotopic shift observed in the present experiments is the same as that reported previously. An absorption at 951.3 cm^{-1}, which has been tentatively attributed to the $(MnO_2)_2$ cluster in a previous report,[6] was observed to exhibit identical behavior upon annealing and irradiation along with the 974.8 cm^{-1} absorption throughout all the experiments. This indicates that the 951.3 and 974.8 cm^{-1} absorptions belong to different vibrational modes of the same molecule. The 951.3 cm^{-1} absorption shifted to 907.5 cm^{-1} when the $^{18}O_2$ sample was used. The resulting $^{16}O/^{18}O$ isotopic ratio of 1.0483 is indicative of a symmetric MnO_2 stretching vibration. The isotopic splittings shown in Figure 3 suggest that the molecule involves a MnO_2 subunit, which is perturbed by another O_2 fragment. A broadband around 1130 cm^{-1} was previously assigned to the O−O stretching mode of the (η^2-O_2)MnO_2 molecule.[6] However, this absorption was not observed in the present experiments. The 974.8 and 951.3 cm^{-1} absorptions increased at the expense of MnO_2. Neither of them can be observed when the sample was annealed directly after sample deposition, during which the manganese dioxide was barely observed. These experimental observations support the assignment of the 974.8 and 951.3 cm^{-1} absorptions to the (η^2-O_2)MnO_2 complex. It is interesting to note that a very weak absorption at 1508.8 cm^{-1} appeared along with the 974.8 and 951.3 cm^{-1} absorptions. The band position and isotopic frequency ratio imply that this absorption is due to an O−O stretching mode of a weakly perturbed dioxygen. This suggests that the (η^2-O_2)MnO_2 complex is perturbed by another dioxygen in forming a van der Waals complex in solid argon.

The structure of MnO_4 has previously been predicted by first-principles calculations based on density functional theory (DFT) and generalized gradient approximation.[13,20] Two structural isomers of C_{2v} symmetry were predicted to be close in energy. The structure with a distorted tetrahedron geometry where all four oxygen atoms are bonded to Mn dissociatively was predicted to be more stable than another isomer in which two of the oxygen atoms remain in a molecular configuration, whereas the other two are dissociated (dioxygen−manganese dioxide complex). To provide additional insight into the spectroscopic assignment of MnO_4 and to provide a prediction of its structure, quantum chemical calculations were performed. At the DFT/B3LYP level of theory, the side-on bonded (η^2-O_2)MnO_2 complex was predicted to have a $^2A_1$ ground state. The end-on bonded (η^1-OO)MnO_2 isomer ($^4A''$) with a nonplanar C_s symmetry lies 7.3 kcal/mol higher in energy than the side-on bonded (η^2-O_2)MnO_2 structure. The distorted tetraoxide structure without O−O bonding was predicted to be 4.4 kcal/mol higher in energy than the side-on bonded (η^2-O_2)MnO_2 isomer, which is in disagreement with previous calculations.[13,20] To further confirm the relative stability of the two structural isomers of MnO_4, single-point energy calculations were per-

TABLE 1: IR Absorptions (cm^{-1}) of the Experimentally Observed (η^2-O_2)MnO_2, (η^2-O_2)MnO_4, and (η^2-O_2)$_2$Mn(μ-O)$_2$Mn Complexes in Solid Argon

$^{16}O_2$	$^{18}O_2$	$^{16}O_2 + {}^{18}O_2$	$^{16}O_2 + {}^{16}O^{18}O + {}^{18}O_2$	mode
		(η^2-O_2)MnO_2		
974.8	937.3	974.8, 937.3		MnO_2 asym. str.
951.3	907.5	951.3, 945.2, 933.0, 907.5		MnO_2 sym. str.
		(η^2-O_2)MnO_4		
1511.7	1426.7	1511.7, 1426.7	1511.7, 1469.8, 1426.7	O_2 str.
959.2	922.1	959.2, 922.1		MnO str.
929.8	891.3	929.8, 927.2, 901.5, 891.3		MnO str.
		(η^2-O_2)$_2$Mn(μ-O)$_2$Mn		
1092.0	1030.5	1096.6, 1091.0, 1034.6, 1030.7	1096.6, 1094.6, 1091.0, 1065.5, 1061.6, 1034.4, 1032.5, 1030.8	O_2 str.
683.6	656.6	683.3, 657.3	683.2, 671.2, 657.1	MnO str.

formed by using the CCSD(T) method with the structures optimized at the B3LYP level of theory. The tetraoxide structure was predicted to be 12.5 kcal/mol higher in energy than the side-on bonded (η^2-O_2)MnO_2 isomer. According to the calculations, the (η^2-O_2)MnO_2 complex has two strong MnO_2 stretching vibrations at 1071.3 and 1040.6 cm^{-1} with comparable IR

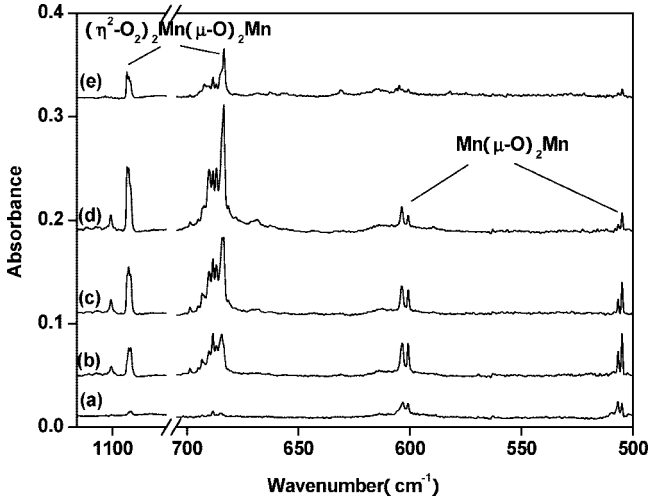

Figure 2. IR spectra in the 1120−1070 and 705−500 cm^{-1} regions from codeposition of laser-evaporated manganese atoms with 0.5% O_2 in argon. (a) 1 h of sample deposition at 6 K, (b) after 25 K annealing, (c) after 30 K annealing, (d) after 35 K annealing, and (e) after 15 min of 250 < λ < 580 nm irradiation.

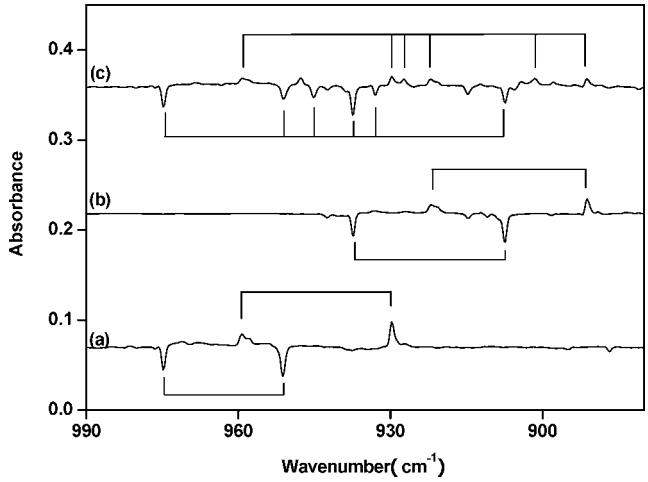

Figure 3. Difference spectra in the 990−880 cm^{-1} region from codeposition of laser-evaporated manganese atoms with isotopic-labeled oxygen in excess argon. (Spectrum taken after 20 min of λ > 500 nm irradiation minus spectrum taken after sample annealing). (a) 1% $^{16}O_2$, (b) 1% $^{18}O_2$, and (c) 0.5% $^{16}O_2$ + 0.5% $^{18}O_2$. Absorptions of (η^2-O_2)MnO_2 are pointing downward, and absorptions of (η^2-O_2)MnO_4 are pointing upward.

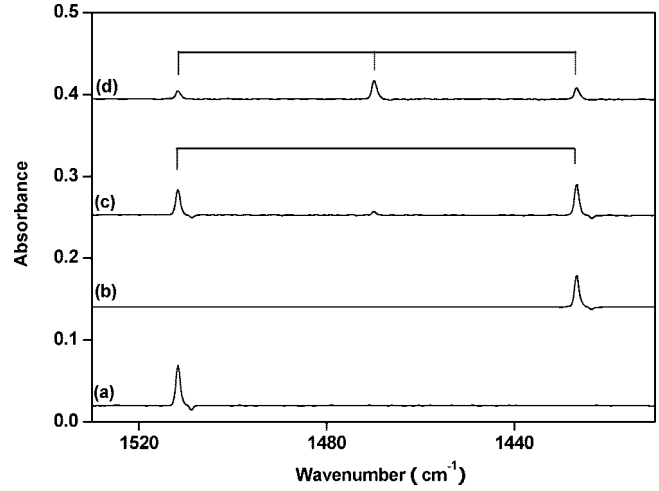

Figure 4. Difference IR spectra in the 1530−1410 cm^{-1} region from codeposition of laser-evaporated manganese atoms with isotopic-labeled oxygen in excess argon. (Spectrum taken after 20 min of λ > 500 nm irradiation minus spectrum taken after sample annealing). (a) 1% $^{16}O_2$, (b) 1% $^{18}O_2$, (c) 0.5% $^{16}O_2$ + 0.5% $^{18}O_2$, and (d) 0.25% $^{16}O_2$ + 0.5% $^{16}O^{18}O$ + 0.25% $^{18}O_2$.

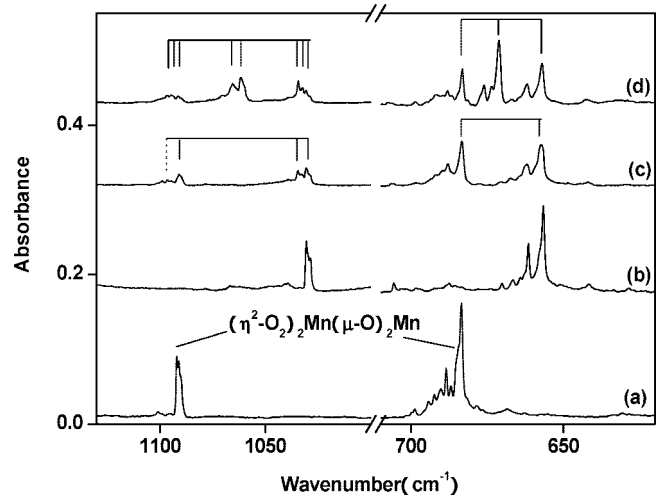

Figure 5. IR spectra in the 1130−1000 and 710−620 cm^{-1} regions from codeposition of laser-evaporated manganese atoms with isotopic-labeled oxygen in excess argon. Spectra were taken after 35 K annealing followed by 15 min of λ,>,500 nm irradiation. (a) 0.5% $^{16}O_2$, (b) 1% $^{18}O_2$, (c) 0.5% $^{16}O_2$ + 0.5% $^{18}O_2$, and (d) 0.25% $^{16}O_2$ + 0.5% $^{16}O^{18}O$ + 0.25% $^{18}O_2$.

TABLE 2: DFT/B3LYP Calculated Total Energies (Hartree), Frequencies (cm^{-1}), and Intensities (km/mol) of the MnO_4, MnO_6, and Mn_2O_6 Species[a]

molecule	energy	frequencies (intensity)
$(\eta^2\text{-}O_2)MnO_2$ ($^2A_1$, C_{2v})	−1451.836389 (−1450.119657)	1071.3 (218), 1040.6 (168), 993.5 (41), 628.3 (13), 584.6 (0), 347.9 (3), 266.9 (1), 262.7 (0), 233.2 (23)
MnO_4 ($^2B_1$, C_{2v})	−1451.829347 (−1450.099743)	1033.2 (130), 1025.9 (80), 808.8 (28), 436.7 (0), 402.7 (1), 359.1 (1), 348.2 (4), 316.6 (0), 285.6 (2)
MnO_4 ($^2B_2$, C_{2v})	−1451.829348 (−1450.099736)	1033.2 (130), 1025.9 (80), 808.5 (28), 436.4 (0), 402.8 (1), 359.1 (1), 348.2 (4), 316.5 (0), 285.6 (2)
$(\eta^2\text{-}O_2)MnO_4$ ($^2A_2$, C_{2v})	−1602.198151	1627.0 (360), 1049.7 (154), 1024.4 (177), 831.1 (89), 581.8 (18), 415.7 (2), 383.0 (3), 373.6 (1), 366.2 (1), 334.9 (0), 316.3 (0), 154.8 (0), 131.7 (0), 116.1 (9), 75.7 (0)
$(\eta^2\text{-}O_2)_2Mn(\mu\text{-}O)_2Mn$ ($^{11}B_{1u}$, D_{2h})	−2753.381731	1185.1 (0), 1178.6 (203), 716.2 (0), 715.3 (678), 643.7 (119), 527.4 (0), 505.6 (0), 459.7 (0), 450.3 (55), 440.7 (1), 255.6 (72), 252.5 (0), 140.0 (0), 133.9 (0), 112.8 (0), 102.6 (0), 84.3 (3), 53.7 (3)

[a] Energy values are given after zero-point energy corrections. The values in parentheses are single-point energies calculated at the CCSD(T)//B3LYP/6-311+G(d) level.

TABLE 3: Comparison between the Observed and Calculated Vibrational Frequencies (cm^{-1}) and Isotopic Frequency Ratios of the Observed Products

	frequencies		$^{16}O/^{18}O$	
mode	calcd	obsd	calcd	obsd
	$(\eta^2\text{-}O_2)MnO_2$			
MnO_2 asym. str. (b_2)	1071.3	974.8	1.0404	1.0400
MnO_2 sym. str. (a_1)	1040.6	951.3	1.0467	1.0483
	$(\eta^2\text{-}O_2)MnO_4$			
O_2 str. (a_1)	1627.0	1511.7	1.0608	1.0596
MnO str. (b_1)	1049.7	959.2	1.0409	1.0402
MnO str. (a_1)	1024.4	929.8	1.0480	1.0432
	$(\eta^2\text{-}O_2)_2Mn(\mu\text{-}O)_2Mn$			
O_2 str. (b_{1u})	1178.6	1092.0	1.0608	1.0597
MnO str. (b_{1u})	715.3	683.6	1.0418	1.0411

intensities (218 versus 168 km/mol, Table 2). The O−O stretching mode was predicted at 993.5 cm^{-1} with much lower IR intensity (43 km/mol) than those of the MnO_2 stretching modes. This mode was not observed in the experiments. As listed in Table 3, both the calculated frequencies and isotopic frequency ratios match well with the experimental values.

As shown in Figure 6, the ground state $(\eta^2\text{-}O_2)MnO_2$ complex has an O−O bond length of 1.399 Å, which is close to that of the recently reported side-on bonded manganese(III) peroxide complex.[32] Therefore, the $(\eta^2\text{-}O_2)MnO_2$ complex can be regarded as $[(MnO_2)^{2+}(O_2^{2-})]$, a side-on bonded peroxo manganese dioxide complex. The complex has a $^2A_1$ ground state with the single occupied molecular orbital mainly being the hybrid of the Mn 4s and $3d_z^2$ orbitals. Consistent with this notion, population analysis shows that the spin density is mainly distributed on the manganese dioxide fragment (1.14 e). The side-on coordination of dioxygen has been observed in many transition-metal systems.[33–35] The structure and bonding of $(\eta^2\text{-}O_2)MnO_2$ is very similar to that of $(\eta^2\text{-}O_2)FeO_2$, which was recently characterized to be a peroxo iron dioxide complex.[35]

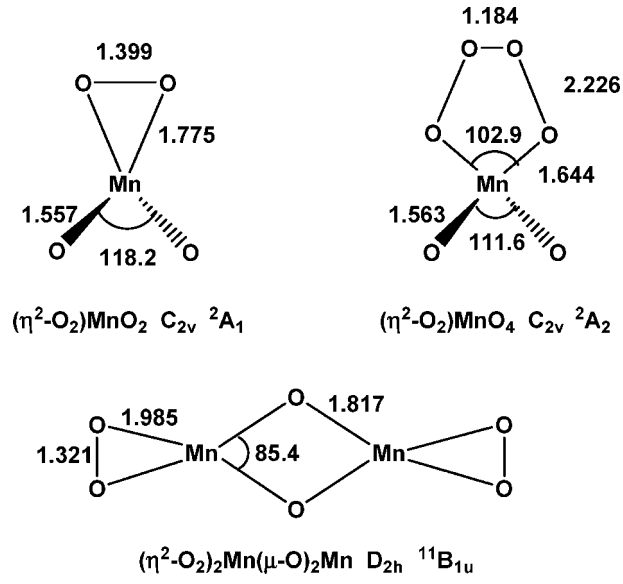

Figure 6. Optimized structures (bond lengths in angstrom and bond angles in degree) of the observed products.

The 951.3 cm^{-1} absorption was tentatively assigned to a Mn_2O_4 cluster in a previous report.[6] DFT calculations predicted that the most stable structure of Mn_2O_4 has a nonplanar C_{2h} symmetry with a cyclic Mn_2O_2 core, similar to that of the recently characterized titanium and chromium dioxide dimers.[36] The observed spectrum does not support the assignment to the Mn_2O_4 cluster.

$(\eta^2\text{-}O_2)MnO_4$. The 1511.7, 959.2, and 929.8 cm^{-1} absorptions appeared upon visible-light irradiation at the expense of the $(\eta^2\text{-}O_2)MnO_2$ complex absorptions. As mentioned above, the $(\eta^2\text{-}O_2)MnO_2$ complex is weakly coordinated by another dioxygen. These experimental observations suggest that the 1511.7, 959.2, and 929.8 cm^{-1} absorptions can be assigned to a species with MnO_6 stoichiometry. The 1511.7 cm^{-1} absorption is unusually strong. The isotopic shifts and splits in the mixed $^{16}O_2 + {}^{18}O_2$ and $^{16}O_2 + {}^{16}O^{18}O + {}^{18}O_2$ experiments (shown in Figure 4) clearly showed that this absorption is due to an O−O stretching vibration with the involvement of only one O_2 fragment having two equivalent O atoms. The 959.2 and 929.8 cm^{-1} absorptions shifted to 922.1 and 891.3 cm^{-1} with the $^{18}O_2$ sample, giving the isotopic $^{16}O/^{18}O$ ratios of 1.0402 and 1.0432, respectively. The observation of two Mn═O stretching modes with similar isotopic $^{16}O/^{18}O$ ratios suggests the involvement of a manganese tetraoxide subunit. Accordingly, we assign the 1511.7, 959.2, and 929.8 cm^{-1} absorptions to the $(\eta^2\text{-}O_2)MnO_4$ complex.

To provide a prediction of its geometric and electronic structure, DFT calculations were performed on the $(\eta^2\text{-}O_2)MnO_4$ complex. On the basis of these calculations, the $(\eta^2\text{-}O_2)MnO_4$ complex has a $^2A_2$ ground state with a C_{2v} symmetry, in which the O_2 fragment is coordinated to two oxygen atoms of the MnO_4 fragment, as shown in Figure 6. The experimentally observed modes were predicted to be 1627.0, 1049.7, and 1024.4 cm^{-1} with 360:154:177 relative IR intensities (Table 2), which are in quite good agreement with the experimental observations.

The $^2A_2$ ground-state (η^2-O_2)MnO_4 complex has two terminal Mn−O bonds with a bond length of 1.563 Å, about 0.033 Å shorter than that of the $^4B_1$ ground-state MnO_2 calculated at the same level of theory. The other two Mn−O bonds possess a relatively longer bond length of 1.644 Å. The O−O bond length of the O_2 fragment is predicted to be 1.184 Å, slightly shorter than the value of molecular oxygen, whereas the O−O distance between the O_2 and MnO_4 fragments is computed to be 2.226 Å, significantly longer than that of typical O−O single bond, and is even longer than that of the H_2OOO^+ cation which was characterized to be a 3c−1e bond.[37] Natural charge population analysis shows that the O_2 fragment is positively charged by about + 0.21 e. However, the (η^2-O_2)MnO_4 complex cannot be regarded as a pure ionic [O_2^+][MnO_4^-] charge-transfer complex. Generally, the O−O stretching vibrational modes of dioxygenyl fluorometallate salts, which were regarded as pure ionic compounds, lie around 1850 cm^{-1}.[38] The O−O stretching frequency of (η^2-O_2)MnO_4 is very close to that of the recently reported $XeOO^+$ cation, which has a strong O−O stretching vibration at 1507.9 cm^{-1} in solid argon.[39] The $XeOO^+$ cation was characterized to involve a (p-π^*) σ bonding between Xe and O_2.

The interaction between O_2 and MnO_4 in (η^2-O_2)MnO_4 is similar to that in the recently reported dioxygen complex of FSO_3 radical.[40] As has been pointed out, although there exists a charge-transfer transition around 360 nm in the UV/vis spectrum, the nature of bonding between the O_2 and FSO_3 fragments cannot be described as a simple charge-transfer complex [O_2^+][FSO_3^-] because of the difference in the electron affinity of FSO_3 and the ionization energy of O_2. The ionization energy of O_2 is 12.063 ± 0.001 eV.[41] The experimental electron affinity of MnO_4 was determined to be only 4.80 ± 0.10 eV,[13] about the same as that of the FSO_3 radical, but is much smaller than that of PtF_6 (7.00 ± 0.35 eV).[42] PtF_6 is well-known to be able to oxidize the O_2 molecule to form the [O_2^+][PtF_6^-] charge-transfer complex.[43]

(η^2-O_2)$_2$Mn(μ-O)$_2$Mn. The 683.6 cm^{-1} absorption was previously assigned to the cyclic Mn(O_2) complex.[6] However, the assignment does not fit theoretical calculations.[6,8b,11] In the present experiments, the 683.6 cm^{-1} absorption increased together with a 1092.0 cm^{-1} absorption at the expense of the cyclic Mn(μ-O)$_2$Mn cluster absorptions. They are reassigned to the (η^2-O_2)$_2$Mn(μ-O)$_2$Mn cluster. The 1092.0 cm^{-1} absorption is due to an O−O stretching vibration. The isotopic spectral features in the mixed $^{16}O_2$ + $^{18}O_2$ and $^{16}O_2$ + $^{16}O^{18}O$ + $^{18}O_2$ experiments (Figure 5) indicate that two equivalent O_2 subunits are involved in this mode. The isotopic shift implies that the 683.6 cm^{-1} absorption is due to a Mn−O stretching mode. The band position and isotopic splitting in the mixed $^{16}O_2$ + $^{18}O_2$ and $^{16}O_2$ + $^{16}O^{18}O$ + $^{18}O_2$ experiments (Figure 5) indicate the involvement of one cyclic Mn(μ-O)$_2$Mn subunit in this mode.

The assignment is confirmed by DFT calculations. As shown in Figure 6, the (η^2-O_2)$_2$Mn(μ-O)$_2$Mn cluster was predicted to have a $^{11}B_{1u}$ ground state with a planar D_{2h} symmetry, in which the Mn_2O_2 core is coordinated by two equivalent O_2 molecules in a side-on fashion. The O−O bond length was predicted to be 1.321 Å with the corresponding IR active vibrational frequency at 1178.6 cm^{-1}. Therefore, the two O_2 subunits are due to superoxide ligands.[33] The (η^2-O_2)$_2$Mn(μ-O)$_2$Mn cluster can be described as [$(O_2^-)_2(Mn_2O_2)^{2+}$], a disuperoxide complex. As can be seen in Table 3, both the calculated frequencies and isotopic frequency ratios are in good agreement with the experimental values.

Reaction Mechanism. The spectra in Figure 1 clearly show that the MnO_2 absorptions increased only under broadband UV−visible light irradiation, which indicates that the formation of inserted MnO_2 from atomic manganese and O_2 requires activation energy. It has been shown in previous experiments that late 3d transition-metal-atom insertion to form the metal dioxide molecules requires photoexcitation.[35,44–47] Subsequent sample annealing allows the O_2 molecules to diffuse and to react with the manganese dioxide to form the side-on bonded peroxo manganese dioxide complex, reaction 1, which was predicted to be exothermic by about 20.2 kcal/mol at the DFT/B3LYP level of theory. The complex absorptions increased on sample annealing, which indicates that this association reaction requires negligible activation energy.

$$MnO_2(^4B_1) + O_2(^3\Sigma_g^-) \rightarrow (\eta^2\text{-}O_2)MnO_2(^2A_1) \qquad \Delta E = -20.2 \text{ kcal/mol} \quad (1)$$

The (η^2-O_2)MnO_4 complex was formed via visible-light (λ > 500 nm) irradiation at the expense of the (η^2-O_2)MnO_2 absorptions. As mentioned above, the (η^2-O_2)MnO_2 complex is weakly coordinated by another molecular oxygen. Hence, the formation of the (η^2-O_2)MnO_4 complex can be rationalized in terms of the isomerization of the (η^2-O_2)MnO_2−O_2 van der Waals complex, reaction 2. According to the DFT/B3LYP calculations, reaction 2 is endothermic by 3.1 kcal/mol. The reaction is assumed to proceed via the initial photoexcitation of the (η^2-O_2)MnO_2 complex, which results in the breaking of the O−O bond to form a metastable manganese tetraoxide. No isolated manganese tetraoxide absorptions were observed, suggesting that manganese tetraoxide is not able to be isolated in solid argon. However, it can be stabilized via another dioxygen coordination in forming the (η^2-O_2)MnO_4 complex.

$$(\eta^2\text{-}O_2)MnO_2\text{−}O_2 \rightarrow (\eta^2\text{-}O_2)MnO_4 \qquad \Delta E = 3.1 \text{ kcal/mol} \quad (2)$$

The manganese tetraoxide neutral is an open-shell species. It has been characterized as a superhalogen with very large electron affinity.[13] The MnO_4^- anion has a closed-shell structure and is thermodynamically and electronically very stable. Apparently, partial charge transfer from dioxygen to MnO_4 in (η^2-O_2)MnO_4 is beneficial to stabilize the complex.

Our experiments also show that the (η^2-O_2)MnO_2−O_2 and (η^2-O_2)MnO_4 complexes are photoreversible. That is, visible-light (λ > 500 nm) irradiation induces the conversion of the (η^2-O_2)MnO_2−O_2 complex to (η^2-O_2)MnO_4, and vice versa with UV−visible-light irradiation (300 < λ < 580 nm).

Metal dimers were also formed on evaporation process and/or on sample annealing as reported previously.[36,48,49] The cyclic Mn(μ-O)$_2$Mn clusters were formed via the spontaneous reaction of manganese dimers with O_2 on sample annealing. Recent investigations have shown that metal dimers are more reactive than metal atoms toward small molecules and are able to activate N_2 and CO.[48,49] The cyclic Mn(μ-O)$_2$Mn cluster further reacted with additional O_2 molecules to give the (η^2-O_2)$_2$Mn(μ-O)$_2$Mn cluster complex, reaction 3, which was predicted to be highly exothermic by about 79.6 kcal/mol. The (η^2-O_2)$_2$Mn(μ-O)$_2$Mn absorptions increasing on annealing indicates that reaction 3 requires negligible activation energy.

$$Mn(\mu\text{-}O)_2Mn(^{11}B_{1u}) + 2O_2(^3\Sigma_g^-) \rightarrow (\eta^2\text{-}O_2)_2Mn(\mu\text{-}O)_2Mn(^{11}B_{1u}) \qquad \Delta E = -79.6 \text{ kcal/mol} \quad (3)$$

Conclusions

The reactions of manganese atoms and dimers with dioxygen have been reinvestigated by using matrix isolation IR spectros-

copy. Three manganese oxide dioxygen complexes were prepared and characterized on the basis of isotopic substitutions as well as theoretical frequency calculations. The manganese atoms react with dioxygen to give the inserted MnO_2 molecules under UV−visible-light irradiation. The MnO_2 molecules react with additional dioxygen to form the $(\eta^2\text{-}O_2)MnO_2$ complex, which is characterized to be a side-on bonded peroxo manganese dioxide complex. The $(\eta^2\text{-}O_2)MnO_2$ complex reacts with another weakly coordinated dioxygen to give the $(\eta^2\text{-}O_2)MnO_4$ complex under visible-light irradiation, in which the manganese tetraoxide is coordinated by a side-on bonded dioxygen. The $(\eta^2\text{-}O_2)MnO_4$ complex decomposes upon UV−visible-light irradiation with the reproduction of the $(\eta^2\text{-}O_2)MnO_2$ complex. Manganese dimer reacts with dioxygen to form the cyclic $Mn(\mu\text{-}O)_2Mn$ cluster spontaneously upon annealing, which further reacts with dioxygen to give the $(\eta^2\text{-}O_2)_2Mn(\mu\text{-}O)_2Mn$ cluster, a side-on bonded disuperoxide complex with a planar D_{2h} structure.

Acknowledgment. Financial support from the National Basic Research Program of China (Grant no. 2007CB815203) and the National Natural Science Foundation of China (Grants no. 20703012 and 20433080) is gratefully acknowledged.

References and Notes

(1) (a) Spence, M. A.; Tomlinson, W. R.; Levy, M. R. *Phys. Chem. Chem. Phys.* **2001**, *3*, 3610. (b) Namiki, K.; Saito, S. *J. Chem. Phys.* **1997**, *107*, 8848.

(2) (a) Adam, A. G.; Azuma, Y.; Li, H.; Merer, A. J.; Chandrakumar, T. *Chem. Phys.* **1991**, *152*, 391. (b) Merer, A. J. *Annu. Rev. Phys. Chem.* **1989**, *40*, 407. (c) Gordon, R. M.; Merer, A. J. *Can. J. Phys.* **1980**, *58*, 642.

(3) Gutsev, G. L.; Rao, B. K.; Jena, P.; Li, X.; Wang, L. S. *J. Chem. Phys.* **2000**, *113*, 1473.

(4) Rudnyi, E. B.; Kaibicheva, E. A.; Sidorov, L. N. *Rapid Commun. Mass Spectrom.* **1993**, *7*, 800.

(5) Ferrante, R. F.; Wilkerson, J. L.; Graham, W. R. M.; Weltner, W., Jr *J. Chem. Phys.* **1977**, *67*, 5904.

(6) Chertihin, G. V.; Andrews, L. *J. Phys. Chem. A* **1997**, *101*, 8547.

(7) (a) Gutsev, G. L.; Andrews, L.; Bauschlicher, C. W., Jr *Theor. Chem. Acc.* **2003**, *109*, 298. (b) Bauschlicher, C. W., Jr.; Maitre, P. *Theor. Chim. Acta* **1995**, *90*, 189.

(8) (a) Gutsev, G. L.; Rao, B. K.; Jena, P. *J. Phys. Chem. A* **2000**, *104*, 5374. (b) Gutsev, G. L.; Rao, B. K.; Jena, P. J. *Phys. Chem. A* **2000**, *104*, 11961.

(9) Dai, B.; Deng, K. M.; Yang, J. L.; Zhu, Q. S. *J. Chem. Phys.* **2003**, *118*, 9608.

(10) Dolg, M.; Wedig, U.; Stoll, H.; Preuss, H. *J. Chem. Phys.* **1987**, *86*, 2123.

(11) Uzunova, E. L.; Nikolov, G. St.; Mikosch, H. *ChemPhysChem* **2004**, *5*, 192.

(12) Cotton, F. A.; Wilkinson, G. *Advanced Inorganic Chemistry*; Wiley-Interscience: New York, 1988.

(13) Gutsev, G. L.; Rao, B. K.; Jena, P.; Wang, X. B.; Wang, L. S. *Chem. Phys. Lett.* **1999**, *312*, 598.

(14) Hendra, P. J. *Spectrochim. Acta* **1968**, *24A*, 125.

(15) Dong, J.; Wang, Y.; Zhou, M. F. *Chem. Phys. Lett.* **2002**, *364*, 511.

(16) (a) Johnson, L. W.; McGlynn, S. P. *Chem. Phys. Lett.* **1971**, *10*, 595. (b) Müller, A.; Diemann, E. *Chem. Phys. Lett.* **1971**, *9*, 369.

(17) Dickson, R. M.; Ziegler, T. *Int. J. Quantum Chem.* **1996**, *58*, 681.

(18) Lee, D. G.; Moylan, C. R.; Hayashi, T.; Brauman, J. I. *J. Am. Chem. Soc.* **1987**, *109*, 3003.

(19) Nakai, H.; Ohmori, Y.; Nakatsuji, H. *J. Phys. Chem.* **1995**, *99*, 8550.

(20) Gutsev, G. L.; Rao, B. K.; Jena, P. *J. Phys. Chem. A* **1999**, *103*, 10819.

(21) Tono, K.; Terasaki, A.; Ohta, T.; Kondow, T. *Chem. Phys. Lett.* **2004**, *388*, 374.

(22) (a) Nayak, S. K.; Jena, P. *J. Am. Chem. Soc.* **1999**, *121*, 644. (b) Nayak, S. K.; Jena, P. *Phys. Rev. Lett.* **1998**, *81*, 2970.

(23) Chiavarino, B.; Crestoni, M. E.; Fornarini, S. *Chem. Eur. J.* **2002**, *8*, 2740.

(24) Pramann, A.; Rademann, K. *Int. J. Mass Spectrom.* **1999**, *185−187*, 673.

(25) Ziemann, P. J.; Castleman, A. W., Jr *Phys. Rev. B* **1992**, *46*, 13480.

(26) Wang, G. J.; Zhou, M. F. *Int. Rev. Phys. Chem.* **2008**, *27*, 1.

(27) Gaussian 03: Frisch, M. J.; Trucks, G. W.; Schlegel, H. B.; Scuseria, G. E.; Robb, M. A.; Cheeseman, J. R.; Montgomery, J. A., Jr.; Vreven, T.; Kudin, K. N.; Burant, J. C.; Millam, J. M.; Iyengar, S. S.; Tomasi, J.; Barone, V.; Mennucci, B.; Cossi, M.; Scalmani, G.; Rega, N.; Petersson, G. A.; Nakatsuji, H.; Hada, M.; Ehara, M.; Toyota, K.; Fukuda, R.; Hasegawa, J.; Ishida, M.; Nakajima, T.; Honda, Y.; Kitao, O.; Nakai, H.; Klene, M.; Li, X.; Knox, J. E.; Hratchian, H. P.; Cross, J. B.; Bakken, V.; Adamo, C.; Jaramillo, J.; Gomperts, R.; Stratmann, R. E.; Yazyev, O.; Austin, A. J.; Cammi, R.; Pomelli, C.; Ochterski, J. W.; Ayala, P. Y.; Morokuma, K.; Voth, G. A.; Salvador, P.; Dannenberg, J. J.; Zakrzewski, V. G.; Dapprich, S.; Daniels, A. D.; Strain, M. C.; Farkas, O.; Malick, D. K.; Rabuck, A. D.; Raghavachari, K.; Foresman, J. B.; Ortiz, J. V.; Cui, Q.; Baboul, A. G.; Clifford, S.; Cioslowski, J.; Stefanov, B. B.; Liu, G.; Liashenko, A.; Piskorz, P.; Komaromi, I.; Martin, R. L.; Fox, D. J.; Keith, T.; Al-Laham, M. A.; Peng, C. Y.; Nanayakkara, A.; Challacombe, M.; Gill, P. M. W.; Johnson, B.; Chen, W.; Wong, M. W.; Gonzalez, C.; Pople, J. A. *Gaussian 03*, revision B.05; Gaussian, Inc.: Wallingford, CT, 2004.

(28) (a) Becke, A. D. *J. Chem. Phys.* **1993**, *98*, 5648. (b) Lee, C.; Yang, W.; Parr, R. G. *Phys. Rev. B* **1988**, *37*, 785.

(29) (a) McLean, A. D.; Chandler, G. S. *J. Chem. Phys.* **1980**, *72*, 5639. (b) Krishnan, R.; Binkley, J. S.; Seeger, R.; Pople, J. A. *J. Chem. Phys.* **1980**, *72*, 650.

(30) Chertihin, G. V.; Andrews, L. *J. Chem. Phys.* **1998**, *108*, 6404.

(31) Zhao, Y. Y.; Gong, Y.; Zhou, M. F. *J. Phys. Chem. A* **2006**, *110*, 10777.

(32) Seo, M. S.; Kim, J. Y.; Annaraj, J.; Kim, Y.; Lee, Y. M.; Kim, S. J.; Kim, J.; Nam, W. *Angew. Chem., Int. Ed.* **2007**, *46*, 377.

(33) (a) Gong, Y.; Zhou, M. F.; Tian, S. X.; Yang, J. L. *J. Phys. Chem. A* **2007**, *111*, 6127. (b) Gong, Y.; Zhou, M. F. *J. Phys. Chem. A* **2007**, *111*, 8973–8979. (c) Gong, Y.; Ding, C. F.; Zhou, M. F. *J. Phys. Chem. A* **2007**, *111*, 11572. (d) Cramer, C. J.; Tolman, W. B.; Theopold, K. H.; Rheingold, A. L. *Proc. Natl. Acad. Sci. U.S.A.* **2003**, *100*, 3635.

(34) Zhai, H. J.; Kiran, B.; Cui, L. F.; Li, X.; Dixon, D. A.; Wang, L. S. *J. Am. Chem. Soc.* **2004**, *126*, 16134.

(35) Gong, Y.; Zhou, M. F.; Andrews, L. *J. Phys. Chem. A* **2007**, *111*, 12001.

(36) (a) Gong, Y.; Zhang, Q. Q.; Zhou, M. F. *J. Phys. Chem. A* **2007**, *111*, 3534. (b) Zhang, Q. Q.; Zhao, Y. Y.; Gong, Y.; Zhou, M. F. *J. Phys. Chem. A* **2007**, *111*, 9775.

(37) Zhou, M. F.; Zeng, A. H.; Wang, Y.; Kong, Q. Y.; Wang, Z. X.; Schleyer, P. V. R. *J. Am. Chem. Soc.* **2003**, *125*, 11512.

(38) (a) Griffiths, J. E.; Sunder, W. A.; Falconer, W. E. *Spectrochim. Acta* **1975**, *31A*, 1207. (b) Edwards, A. J.; Falconer, W. E.; Griffiths, J. E.; Sunder, W. A.; Vasile, M. J. *J. Chem. Soc., Dalton Trans.* **1974**, 1129.

(39) Zhou, M. F.; Zhao, Y. Y.; Gong, Y.; Li, J. *J. Am. Chem. Soc.* **2006**, *128*, 2504.

(40) Beckers, H.; Garcia, P,.; Willner, H.; Argüello, G. A.; Cobos, C. J.; Francisco, J. S. *Angew. Chem., Int. Ed.* **2007**, *46*, 3754.

(41) *CRC Handbook of Chemistry and Physics*; CRC Press: Boca Raton, FL, 1985.

(42) Kuznetsov, S. V.; Korobov, M. V.; Sidorov, L. N.; Shipachev, V. A.; Mitkin, V. N. *Int. J. Mass Spectrom. Ion Processes* **1989**, *87*, 13.

(43) Bartlett, N. *Proc. Chem. Soc.* **1962**, 218.

(44) (a) Andrews, L.; Chertihin, G. V.; Ricca, A.; Bauschlicher, C. W., Jr *J. Am. Chem. Soc.* **1996**, *118*, 467. (b) Chertihin, G. V.; Saffel, W.; Yustein, J. T.; Andrews, L.; Neurock, M.; Ricca, A.; Bauschlicher, C. W., Jr *J. Phys. Chem.* **1996**, *100*, 5261.

(45) Chertihin, G. V.; Citra, A.; Andrews, L.; Bauschlicher, C. W., Jr *J. Phys. Chem. A* **1997**, *101*, 8793.

(46) Citra, A.; Chertihin, G. V.; Andrews, L.; Neurock, M. *J. Phys. Chem. A* **1997**, *101*, 3109.

(47) (a) Danset, D.; Alikhani, M. E.; Manceron, L. *J. Phys. Chem. A* **2005**, *109*, 97. (b) Allouti, F.; Manceron, L.; Alikhani, M. E. *Phys. Chem. Chem. Phys.* **2006**, *8*, 448.

(48) (a) Zhou, M. F.; Jin, X.; Gong, Y.; Li, J. *Angew. Chem., Int. Ed.* **2007**, *46*, 2911. (b) Gong, Y.; Zhao, Y. Y.; Zhou, M. F. *J. Phys. Chem. A* **2007**, *111*, 6204. (c) Zhou, M. F.; Jin, X.; Li, J. *J. Phys. Chem. A* **2006**, *110*, 10206. (d) Jin, X.; Jiang, L.; Xu, Q.; Zhou, M. F. *J. Phys. Chem. A* **2006**, *110*, 12585.

(49) (a) Himmel, H. J.; Hübner, O.; Klopper, W.; Manceron, L. *Angew. Chem., Int. Ed.* **2006**, *45*, 2799. (b) Himmel, H. J.; Hübner, O.; Bischoff, F. A.; Klopper, W.; Manceron, L. *Phys. Chem. Chem. Phys.* **2006**, *8*, 2000. (c) Kuganathan, N.; Green, J. C.; Himmel, H. J. *New J. Chem.* **2006**, *30*, 1253.

JP800955E